# Investigation into the dehydration of selenate doped $Na_2M(SO_4)_2 \cdot 2H_2O$ (M = Mn, Fe, Co and Ni): stabilisation of the high Na content alluaudite phases $Na_3M_{1.5}(SO_4)_{3-1.5x}(SeO_4)_{1.5x}$ (M = Mn, Co and Ni) through selenate incorporation

Driscoll, Laura; Kendrick, Emma; Knight, Kevin S.; Wright, Adrian; Slater, Peter

*DOI:*
10.1016/j.jssc.2017.09.025



*Document Version*
Peer reviewed version

*Citation for published version (Harvard):*
Driscoll, L, Kendrick, E, Knight, KS, Wright, A & Slater, P 2018, 'Investigation into the dehydration of selenate doped $Na_2M(SO_4)_2 \cdot 2H_2O$ (M = Mn, Fe, Co and Ni): stabilisation of the high Na content alluaudite phases $Na_3M_{1.5}(SO_4)_{3-1.5x}(SeO_4)_{1.5x}$ (M = Mn, Co and Ni) through selenate incorporation', *Journal of Solid State Chemistry*. https://doi.org/10.1016/j.jssc.2017.09.025

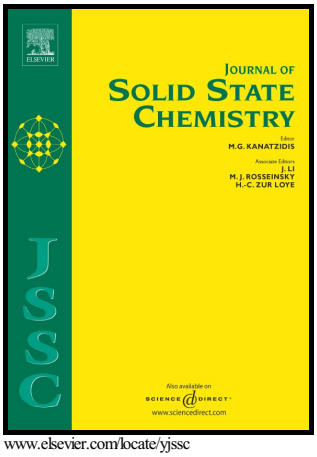


www.elsevier.com/locate/yjssc

# Investigation into the dehydration of selenate doped $Na_2M(SO_4)_2{\cdot}2H_2O$ (M = Mn, Fe, Co and Ni): stabilisation of the high Na content alluaudite phases $Na_3M_{1.5}(SO_4)_{3-x}(SeO_4)_x$ (M = Mn, Co and Ni) through selenate incorporation

L.L. Driscoll, E. Kendrick, K.S. Knight, A.J. Wright, P.R. Slater

PII: S0022-4596(17)30382-1
DOI: http://dx.doi.org/10.1016/j.jssc.2017.09.025
Reference: YJSSC19955

To appear in: *Journal of Solid State Chemistry*

Received date: 2 August 2017
Revised date: 20 September 2017
Accepted date: 23 September 2017

Cite this article as: L.L. Driscoll, E. Kendrick, K.S. Knight, A.J. Wright and P.R. Slater, Investigation into the dehydration of selenate doped $Na_2M(SO_4)_2{\cdot}2H_2O$ (M = Mn, Fe, Co and Ni): stabilisation of the high Na content alluaudite phases $Na_3M_{1.5}(SO_4)_{3-x}(SeO_4)_x$ (M = Mn, Co and Ni) through selenate incorporation, *Journal of Solid State Chemistry,* http://dx.doi.org/10.1016/j.jssc.2017.09.025

# Investigation into the dehydration of selenate doped $Na_2M(SO_4)_2 \cdot 2H_2O$ (M = Mn, Fe, Co and Ni): stabilisation of the high Na content alluaudite phases $Na_3M_{1.5}(SO_4)_{3-x}(SeO_4)_x$ (M = Mn, Co and Ni) through selenate incorporation

L.L. Driscoll[1*], E. Kendrick[1,2], K.S. Knight[3,4] A. J. Wright[1] and P.R. Slater[1*]

[1]School of Chemistry, University of Birmingham, Edgbaston, Birmingham, West Midlands B15 2TT

[2] WMG, University of Warwick, Coventry, CV4 7AL

[3]Department of Earth Sciences, University College London, Gower Street, London, WC1E 6BT, U.K.

[4] Department of Earth Sciences, The Natural History Museum, Cromwell Road, London, SW7 5BD, U.K.

Correspondence to:

Dr. L.L. Driscoll or

Prof. P.R. Slater

School of Chemistry, University of Birmingham, Edgbaston, Birmingham, West Midlands B15 2TT

l.l.driscoll@bham.ac.uk or

p.r.slater@bham.ac.uk

**Abstract**

In this paper we report an investigation into the phases formed on dehydration of $Na_2M(SO_4)_{2-x}(SeO_4)_x \cdot 2H_2O$ ($0 \leq x \leq 1$; M = Mn, Fe, Co and Ni). For the Fe series, all attempts to dehydrate the samples doped with selenate resulted in amorphous products, and it is suspected that a side redox reaction involving the Fe and selenate may be occurring leading to phase decomposition and hence the lack of a crystalline product on dehydration. For M = Mn, Co, Ni, the structure observed was shown to depend upon the transition metal cation and level of selenate doping. An alluaudite phase, $Na_3M_{1.5}(SO_4)_{3-1.5x}(SO_4)_{1.5x}$, was observed for the selenate doped compositions, with this phase forming as a single phase for $x \geq 0.5$ M = Co, and x = 1.0 M = Ni. For M = Mn, the alluaudite structure is obtained across the series, albeit with small impurities for lower selenate content samples. Although the alluaudite-type phases $Na_{2+2y}(Mn/Co)_{2-y}(SO_4)_3$ have recently been reported [1,2], doping with selenate appears to increase the maximum sodium content within the structure. Moreover, the selenate doped Ni based samples reported here are the first examples of a Ni sulfate/selenate containing system exhibiting the alluaudite structure.

**Keywords**: Sodium ion, Sulfate, Selenate, alluaudite, Crystal Structure

## Introduction

There is growing interest in the structures and properties of mineral systems constructed from metal octahedra and oxoanion tetrahedra. This research interest has been driven by potential applications in a number of technologically important areas, including applications as battery electrodes [3–7], fuel cell materials [8–13], medical applications [14],[15] and pigments[16]. Recently the Na transition metal sulfate hydrate systems, $Na_2M(SO_4)_2.2H_2O$ (M = transition metal) have attracted interest following reports on the use of $Na_2Fe(SO_4)_2 \cdot 2H_2O$ as a potential electrode material for Na ion batteries [2]. In a recent paper, we investigated the partial substitution of $SeO_4^{2-}/PO_3F^{2-}$ for $SO_4^{2-}$ in these $Na_2M(SO_4)_2.2H_2O$ (M = transition metal) systems, and showed how the incorporation of these alternative tetrahedral units could cause significant alterations to the structure obtained[17]. Of further interest is the effect this doping strategy has on the resultant products obtained from the dehydration of these dihydrates. For example, dehydration of $Na_2M(SO_4)_2.2H_2O$ (M = Fe) has been shown to produce a material with the alluaudite-type structure, which also shows good performance as a Na ion battery electrode material[18]. Reports regarding the alluaudite system often refer to off-stoichiometric behaviour, with compositions such as $Na_{2+2y}Fe_{2-y}(SO_4)_3$ ($y \leq 0.3$) common for this material.[19,20] Similar formation of an alluadite-type phase has been observed on dehydration of the Mn based system[2], while for the M = Ni, Co systems dehydration leads to the formation of the simple bimetallic sulfate $Na_2M(SO_4)_2$ [6].We have therefore extended our studies on $Na_2M(SO_4)_{2-x}(SeO_4)_x/(PO_3F)_x.2H_2O$ systems to determine whether there are any differences in the phases ($Na_2M(SO_4)_2$- or alluaudite-type) formed on dehydration of these doped systems. Furthermore, the synthesis of such $Na_2M(SO_4)_2$- or alluaudite-type phases via the dehydration of $Na_2M(SO_4)_{2-x}(SeO_4)_x/(PO_3F)_x.2H_2O$ prepared by a simple initial solution step not only reduces the synthesis time, by avoiding the need for prolonged milling and/or lengthy heating times, but also offers a low temperature route to obtain these

phases, which are prone to decomposition at elevated temperatures. Unfortunately, in the case of the $PO_3F$ doped samples, the dehydration experiments led to significant impurities, suggesting decomposition of the fluorophosphate unit after thermal treatment. In contrast, dehydration of the selenate doped samples were successful, and in this paper we present the results from the dehydration of the $Na_2M(SO_4)_{2-x}(SeO_4)_x \cdot 2H_2O$ (M = Fe, Co, Mn, Ni; $0 \leq x \leq 1.0$) materials, illustrating the significant effect of the incorporation of selenate on the products obtained.

**Experimental**

For ease of preparation and high purity of the resultant samples, the sodium transition metal sulfate hydrates were synthesized via a wet chemical route, as described earlier [17]. Briefly, stoichiometric amounts of $MSO_4 \cdot yH_2O$ (Sigma Aldrich, 99%) (where M = Mn, Fe, Co, Ni and Cu, y = 1 for Fe and Mn, 5 for Cu, 6 for Ni and 7 for Co) and sodium sulfate (Sigma Aldrich, 99%) were dissolved in water (for the Fe samples, ascorbic acid was added to the solutions in order to prevent oxidation of $Fe^{2+}$ to $Fe^{3+}$). After mixing at 60°C for 30 minutes, the samples were then placed in an oven and evaporated to dryness at 60-110°C for Mn, Fe, and Co samples and 130°C for Ni. The $Na_2M(SO_4)_{2-x}(SeO_4)_x \cdot 2H_2O$ samples (where M = Mn, Fe, Co, Ni) were synthesized using the same solution method, where sodium selenate was used in place of $Na_2SO_4$ as the selenate source (the maximum level of doping examined was 50% substitution (i.e. x = 1)). Dehydration of the obtained dihydrates was performed by heating the samples at a rate of 0.5°C $min^{-1}$ to 300-350°C, and holding at this temperature for 12 hours in air (or nitrogen for air sensitive samples (M = Fe)).

Thermogravimetric studies were conducted using a Netzsch STA 449 F1 Jupiter thermogravimetric analyser coupled with a Netzsch 403C mass spectrometer (heating rate of 0.5°C $min^{-1}$ under a nitrogen atmosphere). Sample purity and unit cell parameters were

determined from powder X-ray diffraction using a Bruker D2 phaser (Co Kα radiation) operating in reflection mode. Structural determination was performed using X-ray diffraction data, with one system analysed through neutron diffraction (data collected using HRPD (High Resolution Powder Diffractometer, ISIS Facility, Rutherford Appleton Laboratory, UK)). Structure refinements were carried out using the GSAS suite of programs using the structural models proposed by Tarascon *et al.* for $Na_2M(SO_4)_2$ and Barpanda *et. al* for the alluaudite phases[6,18,21,22]. Further characterisation of these systems was performed using Raman spectroscopy (Renishaw in Via Raman microscope equipped with a He-Ne 633 nm laser).

**Results**

The results of the thermogravimetric study (see supplementary information – Figure 1) show that all samples exhibit the ~10% mass loss associated with the loss of two moles of water, as expected for these dihydrates. For both cobalt and nickel systems, the TG results indicated that the dehydration temperature of the selenate doped systems increased with increasing selenate concentration (an increase of 50°C from x=0 (~200°C) to x=1.0 (~250°C) in the Ni system). Samples which are doped with selenate are, however, not as thermally stable at elevated temperatures when compared to the undoped sulfates. The sulfates appear to be stable up to at least 600°C, whereas selenate doped samples decompose in the region of 450-500°C. The mass losses in this region for the latter samples are believed to be attributed to the decomposition of the selenate oxoanion. From the results of the TG studies, samples were heated to 350°C to ensure complete removal of structural water.

The structures resulting from dehydration differ significantly to those of the starting hydrated phases, as the structure directing water molecules are lost. For the sulfate endmember $Na_2M(SO_4)_2 \cdot 2H_2O$, dehydration of both Co and Ni systems resulted in the bimetallic sulfate $Na_2M(SO_4)_2$ (M=Co, Ni) as shown previously by Tarascon et al. [6] (**Figure 1**). In contrast,

dehydration of $Na_2M(SO_4)_2 \cdot 2H_2O$ (M=Mn, Fe), led to the formation of an alluaudite type phase along with some impurities, as recently shown by Marinova et al[23]. For the Fe series, all attempts to dehydrate the samples doped with selenate resulted in amorphous products, and so the phase composition of the selenate doped Fe samples could not be analysed by X-ray diffraction. It is suspected that a side redox reaction involving the Fe and selenate may be occurring within the material, due to the oxidising power of selenate ($Se^{VI} \rightarrow Se^{IV}$), which may be leading to phase decomposition and hence the lack of a crystalline product on dehydration.

We discuss here in detail the structural properties of the dehydrated phases for selenate-doped $Na_2M(SO_4)_{2-x}(SeO_4)_x \cdot 2H_2O$ (M = Co, Mn, Ni; $0 \leq x \leq 1.0$).

**Dehydration results for $Na_2Co(SO_4)_{2-x}(SeO_4)x \cdot 2H_2O$ ($0 \leq x \leq 1.0$)**

While dehydration of the sulfate endmember led to the formation of the simple bimetallic sulfate $Na_2Co(SO_4)_2$, samples containing selenate, $Na_2Co(SO_4)_{2-x}(SeO_4)_x$, showed a two phase mixture for selenate concentration up to 25% (x = 0.5). This mixture consisted of the sulfate phase $Na_2Co(SO_4)_2$, and a second new phase, whose X-ray diffraction pattern resembled that of alluaudite-type $Na_{2+2y}Mn_{2-y}(SO_4)_3$. The second phase Bragg peaks increased in intensity with increasing selenate content, and for $x \geq 0.5$, a single phase alluaudite-type phase was obtained. (**Figure 2**). Notably, this is the first reported alluadite-type phase for bimetallic mixed sulfate selenates. A further key feature to note is the high Na:Co ratio of 2:1 in the present samples, whereas normally (for alluaudite) the ratio of the metal cations is closer to 1:1. Therefore, in order to clarify this difference, the structure of $Na_2Co(SO_4)(SeO_4)$ was elucidated using neutron diffraction.

Initially the occupancies of all Na and Co sites were freely refined to confirm the stoichiometry of this new alluaudite-type phase. In these initial refinements, the occupancy of

the Co1 site, in particular, showed a significant increase above 1. This suggested some Na was present on these sites due to the larger neutron scattering length of Na compared with Co. The presence of Na on the cobalt sites was checked by a further structure refinement where Na (total site occupancy constrained to 1) was allowed to be present on both Co1 and Co2 sites. This refinement indicated an approximate 50:50 occupancy of Co and Na on the Co1 site (Co:Na occupancy = 0.46:0.54). In contrast, the Co occupancy on the Co2 site did not substantially deviate from 1 with the refinement indicating negligible Na on this site. Therefore, the occupancy of the Co1 site was fixed at 0.5Co:0.5Na, while the Co2 occupancy was constrained as fully occupied by Co. The refinement of the occupancies of the Na1 and Na2 sites, gave values which did not deviate significantly from 1.0, suggesting both sites were fully occupied by Na. A third partially occupied Na site, Na3, has also been reported for the alluaudite structure, and the occupancy of this Na site refined to ≈0.5. The S/Se occupancies were also refined but these did not deviate significantly from the nominal expected composition of 0.5:0.5 S:Se for each site. Therefore the composition for this structural model is $Na_3Co_{1.5}(SO_4)_{1.5}(SeO_4)_{1.5}$, which is consistent with the Na:Co:Se:S ratio of 2:1:1:1 of the starting $Na_2Co(SO_4)(SeO_4).2H_2O$ hydrated phase. Hence the observation of the alluaudite structure with this high Na:Co ratio appears to be related to significant additional occupancy of one of the Co sites by Na. The final refined structural parameters are shown in Table 1 (the resulting observed, calculated, and difference plots for the separate X-ray and neutron diffraction structure refinements using this structural model are shown in **Figure 3**).

Both $Na_2Co(SO_4)_2$ and alluaudite-type $Na_3Co_{1.5}(SO_4)_{1.5}(SeO_4)_{1.5}$ structures are built of a network of distorted metal octahedra and sulfate/selenate tetrahedra. In $Na_2Co(SO_4)_2$, the framework is constructed of metal octahedra that corner and edge share with the sulfate tetrahedra (**Figure 1**). The sodium ions are dispersed throughout the structure in the cavities created by the framework. The structure of alluaudite-type $Na_3Co_{1.5}(SO_4)_{1.5}(SeO_4)_{1.5}$ differs

significantly from the $Na_2Co(SO_4)_2$ phase (**Figure 4**). In the alluaudite case, the metal octahedra bond to the sulfate/selenate tetrahedra through only corner-sharing. The metal octahedra form chains bridged by the sulfate/selenate tetrahedra along the *b*-axis (S1/Se1 bridge Co2, S2/Se2 bridge Co1). These chains then stack and alternate along the *a*-axis, separated by the third sulfate/selenate tetrahedra (S3/Se3). The Co1 site, which is half occupied by sodium, shows a large degree of distortion from the ideal octahedral geometry, which can be related to the mixed cation occupancy of this site. The remaining sodium ions are located within channels in the framework (Na2 and Na3), or between the tetrahedra that bridge the metal octahedra bi-units (Na1).

After successfully solving the structure of this new phase with neutron diffraction, the structural model was applied to the rest of the series to analyse the X-ray diffraction data. As noted earlier, the samples of $Na_2Co(SO_4)_{2-x}(SeO_4)_x$ with $x<0.5$ consisted of two phases, and so a two phase refinement was performed to determine the cell parameters of the individual phases, and the approximate phase fraction. The results from these structure refinements are summarized in Table 2 (Observed, calculated and difference X-ray diffraction plots are shown in supplementary information). The data show an increase in cell parameters on selenate doping across the alluaudite series as expected due to the larger size of the selenate versus the sulfate tetrahedron.



**Dehydration results for $Na_2Ni(SO_4)_{2-x}(SeO_4)x\cdot 2H_2O$ ($0 \leq x \leq 1.0$)**

For the Ni series, $Na_2Ni(SO_4)_{2-x}(SeO_4)_x\cdot 2H_2O$ ($0\leq x\leq 1.0$), a slightly different series of products was observed on dehydration. In this system, at low selenate levels ($x\leq 0.25$), dehydration led to the formation of the simple bimetallic sulfate $Na_2Ni(SO_4)_{2-x}(SeO_4)_x$. On increasing the selenate content further ($x=0.5$ and 0.75 samples), a two phase mixture was

observed as for the selenate doped Co systems. For the highest selenate level analysed (x=1.0), a single phase alluaudite sample was then observed (**Figure 5**). Using the structural models for the alluaudite-type phase from the Co-based system and that for $Na_2Ni(SO_4)_2$, dual phase refinements (X-ray diffraction data) were conducted for this Ni series (Table 3; observed, calculated and difference X-ray diffraction plots are shown in supplementary information). The results indicate that at low selenate levels, the selenate is successfully accommodated in the simple 212 structure, $Na_2Ni(SO_4)_{2-x}(SeO_4)_x$ ($x \leq 0.25$), with the cell parameters shown to increase as expected with increasing selenate content. On further increase, the alluaudite phase starts to appear and a dual phase mixture is observed. The cell parameters of the alluaudite phase increase with increasing selenate content, up to x=1.0 when a single phase alluaudite sample is obtained.

**Dehydration results for $Na_2Mn(SO_4)_{2-x}(SeO_4)_x \cdot 2H_2O$ ($0 \leq x \leq 1.0$)**

As noted earlier, dehydration of undoped $Na_2Mn(SO_4)_2 \cdot 2H_2O$ leads to the formation of an alluaudite-type phase. Thus, contrary to the Co, Ni based systems, the dehydrated "$Na_2Mn(SO_4)_2$" phase, appears to naturally adopt the alluaudite framework without the need for selenate doping. However, the resultant X-ray diffraction pattern showed the presence of impurity phases after dehydration (identified by black diamonds in **Figure 6**). Of note, however, is that, when the concentration of selenate is increased, the impurity phases appear to decrease until these impurities are no longer present once the selenate dopant level reaches x = 0.5 in the starting dihydrate. Cell parameters obtained from structure determination (X-ray diffraction data) using the alluaudite structural model are summarized in Table 4 (observed, calculated and difference X-ray diffraction plots generated from the structure refinement for these dehydrated phases can be found in supplementary information).

The cell volumes for these alluaudite phases are plotted against the selenate concentration in the starting dihydrate phases in **Figure 7**. For the Mn series, for which the alluaudite structure is observed for all compositions, the cell volume increases with increasing selenate content across the series. However, the variation is not quite linear, with a small change in slope apparent at x=0.5. This is consistent with phases, which have a selenate content lower than this value showing the presence of small unidentified impurities, while samples with higher selenate content were single phase. Similar increases in cell volume with selenate content were observed for the Co, Ni containing alluaudite phases, albeit with small variations from linearity associated with the formation of mixed phases for some of the lower selenate content samples.

**Raman data for dehydrated $Na_2M(SO_4)_{2-x}(SeO_4)_x \cdot 2H_2O$ (M = Mn, Co and Ni)**

The samples obtained through the dehydration of the dihydrates were also analysed by Raman spectroscopy to observe the nature of the oxoanion (sulfate/selenate) bonding in the material (**Figure 8**). The undoped $Na_2Ni(SO_4)_2$ sample shows a much more complicated Raman spectrum compared with that of a sample that has adopted the alluaudite structure. The origin of the additional peaks could be due to the bonding of the sulfate oxoanion; in $Na_2M(SO_4)_2$, two oxygens in the sulfate tetrahedron edge share with the metal octahedra. This bonding leads to a decrease in the overall symmetry of the sulfate anion, leading to the formation of four bands in the Raman spectrum in the region of 950-1050 $cm^{-1}$[24],[25]. The Raman spectra for the alluaudite phase shows a single broad band in this region, which can be seen clearly for the Mn systems which naturally adopts the alluaudite structure, both with and without selenate doping. A similar band at lower wavenumber (800-900 $cm^{-1}$), which increases in intensity with increasing selenate content, is observed for the selenate group. Although still behaving as bidentate ligands, the sulfate/selenate in the alluaudite structure now bridges the octahedra through corner-sharing, as opposed to edge-sharing. This

difference in spectra provides additional evidence of the formation of a single phase material with the alluaudite structure with increasing selenate content for M=Ni, Co. The Raman data are in good agreement with the diffraction data obtained for these phases; in particular the Co system shows very little evidence of the $Na_2M(SO_4)_2$ phase when x>0.25-0.5. The Ni spectra not only show the transformation from a $Na_2M(SO_4)_2$ type phase to $Na_3M_{1.5}(SO_4)_{1.5}(SeO_4)_{1.5}$, but also provide evidence that the $(SeO_4)^{2-}$ anion has entered the $Na_2Ni(SO_4)_2$ structure as the peaks in the selenate region appear to, although broad, mimic those of the sulfate region of $Na_2Ni(SO_4)_2$; i.e. at least two peaks can be distinguished in this range for the x = 0.25 sample whereas the $(SeO_4)^{2-}$ band in the alluaudite phase appears to be singular and very broad. A very subtle shift of the $(SO_4)^{2-}$ peaks to lower wavenumber is also observed, suggesting weakening of the S-O bond in the alluaudite phase with increasing selenate concentration from x=0.5 to x=1.0, consistent with selenate incorporation.

**Discussion**

The products observed after dehydration of $Na_2M(SO_4)_2 \cdot 2H_2O$ (M = Mn, Fe, Co and Ni) indicate that smaller cations such as $Co^{2+}$ and $Ni^{2+}$ favour formation of the $Na_2Co(SO_4)_2$ structure, whereas larger cations such as $Mn^{2+}$ and $Fe^{2+}$ prefer to adopt the alluaudite framework, $Na_2M_2(SO_4)_3$. The origin of this structural preference may be a consequence of the bonding in $Na_2M(SO_4)_2$, in which edge-sharing of metal octahedra and sulfate tetrahedra are utilized to form the structure. Such edge-sharing means that the central cations of the two sites are closer to each other than for a structure containing only corner linked octahedra and tetrahedra. For larger cations, it could be suggested that doping the tetrahedral site with the larger selenate oxyanion causes edge sharing to become unfavorable in the $Na_2M(SO_4)_2$ structure under standard conditions and therefore formation of the alluaudite structure is preferred. In this respect, to date, there appears to be no literature reporting the synthesis of $Na_2Mn(SO_4)_2$ and only one report of $Na_2Fe(SO_4)_2$, indicating the difficulty in synthesizing

these phases, with formation of the alluaudite preferred [6]. The adoption of the alluaudite framework in Co and Ni systems after doping the system with selenate suggests that the edge sharing between the larger selenate on the tetrahedral site and the metal octahedra becomes even more unfavourable and therefore selenate doping favours the alternative alluaudite-type structure. To support this theory, the sum of the ionic radii of M (where M = Mn, Co and Ni) and the weighted average ionic radii of X (where X = S/Se) has been plotted against the selenate content in the starting dihydrate phase. Labels indicating the phases formed after dehydration have also been added to the plot. The plot (**Figure 9**) shows a good correlation between this sum of the sizes of the transition metal and the weighted average S/Se size, and the subsequent phase obtained after dehydration. From these results it is apparent that it is both the size of the transition metal and the selenate content that dictates the structure obtained. In order to obtain the alluaudite phase after dehydration, a greater selenate concentration is required as the size of the transition metal decreases (Co (0.745 Å) forms alluaudite for x = 0.5, whereas Ni (0.69 Å) forms alluaudite for x=1.0). Notably this indication that the size of the tetrahedral cation can be exploited to stabilise the alluaudite structure suggests further work is warranted in this area to access new alluaudite systems.

A further significant result from this study is the higher Na content achievable in these selenate-doped alluaudite phases. The dehydration of the simple sulfate $Na_2Mn(SO_4)_2.2H_2O$ leads to the observation of impurities in addition to the alluaudite-type phase. The presence of these impurities can be related to the high Na:Mn ratio (2:1) in the parent dihydrate, which is significantly higher than the ideal Na:Mn (1:1) ratio in ideal stoichiometric alluaudite $Na_2Mn_2(SO_4)_3$. It should be noted, however, that recent work on such Mn, Fe, Co containing alluaudite systems have indicated that the alluaudite structure may accommodate a degree of non-stoichiometry with a tendency towards higher Na:Mn/Fe/Co ratios, such that the formula should be written $Na_{2+2y}(Mn/Fe/Co)_{2-y}(SO_4)_3$ ($0<y<0.26$). Nevertheless, the Na content limit

reported so far in the literature, for M = Mn, Fe and Co, has been <2.52[1,26–28] Significantly, the results presented here show that, on selenate doping, the impurity phases are eliminated leading to the formation of the very high Na content alluaudite systems $Na_3M_{1.5}(SO_4)_{3-x}(SeO_4)_x$.

Therefore, the results indicate that phases formed in these mixed metal oxoanion series can be manipulated through both changes on the metal and oxoanion sites, indicating multiple avenues for the design of new chemical systems. In particular, selenate incorporation appears to raise the Na content achievable for these alluaudite systems, and allow the formation of alluaudite systems for smaller transition metals.

## Conclusions

In this paper we have reported the successful synthesis of a range of phases resulting from the dehydration of $Na_2M(SO_4)_{2-x}(SeO_4)_x \cdot 2H_2O$ (M=Mn, Co, Ni; $0 \leq x \leq 1.0$). The structure observed was shown to depend upon the transition metal cation and level of selenate doping. An alluaudite phase was observed in selenate doped compositions, with this phase forming as a single phase for $x \geq 0.5$ Co and $x = 1.0$ Ni. For M=Mn, the alluaudite structure is obtained across the series, albeit with small impurities for lower selenate content samples. Although the undoped Mn phase has been reported in the literature recently[2], doping with selenate appears to increase the maximum sodium content within the structure. Moreover, the selenate doped Ni based samples reported here are the first examples of a Ni sulfate containing system exhibiting the alluaudite structure. Overall the results show that doping on the oxoanion site can allow the stabilisation of new alluaudite systems with higher Na contents and smaller transition metals.



## Acknowledgements

We would like to thank the Midlands Energy Consortium for funding (studentship to LD). The Bruker diffractometer, Retsch Raman microscope used in this research was obtained, through Birmingham Science City: Creating and Characterising Next Generation Advanced Materials (West Midlands Centre for Advanced Materials Project 1), with support from Advantage West Midlands (AWM) and part funded by the European Regional Development Fund (EDRF). The Advanced Materials Facility is part of the Centre for Chemical and Materials Analysis in the School of Chemistry at the University of Birmingham. We would like to also thank ISIS at the Rutherford Appleton Laboratory for the provision of neutron diffraction beam time.

References

[1] D. Dwibedi, R. Gond, A. Dayamani, R.B. Araujo, S. Chakraborty, R. Ahuja, P. Barpanda, $Na_{2.32}Co_{1.84}(SO_4)_3$ as a new member of the alluaudite family of high-voltage sodium battery cathodes, Dalt. Trans. 46 (2017) 55–63. doi:10.1039/C6DT03767D.

[2] D. Dwibedi, R.B. Araujo, S. Chakraborty, P.P. Shanbogh, N.G. Sundaram, R. Ahuja, P. Barpanda, $Na_{2.44}Mn_{1.79}(SO_4)_3$: a new member of the alluaudite family of insertion compounds for sodium ion batteries, J. Mater. Chem. A. 3 (2015) 18564–18571. doi:10.1039/C5TA04527D.

[3] G. Rousse, J.M. Tarascon, Sulfate-Based Polyanionic Compounds for Li-Ion Batteries: Synthesis, Crystal Chemistry, and Electrochemistry Aspects, Chem. Mater. 26 (2014) 394–406. doi:10.1021/cm4022358.

[4] P. Barpanda, Sulfate Chemistry for High-Voltage Insertion Materials: Synthetic, Structural and Electrochemical Insights, Isr. J. Chem. 55 (2015) 537–557. doi:10.1002/ijch.201400157.

[5] C. Masquelier, L. Croguennec, Polyanionic (phosphates, silicates, sulfates) frameworks as electrode materials for rechargeable Li (or Na) batteries, Chem. Rev. 113 (2013) 6552–6591. doi:10.1021/cr3001862.

[6] M. Reynaud, G. Rousse, A.M. Abakumov, M.T. Sougrati, G. Van Tendeloo, J.-N. Chotard, J.-M. Tarascon, Design of new electrode materials for Li-ion and Na-ion batteries from the bloedite mineral $Na_2Mg(SO_4)_2 \cdot 4H_2O$, J. Mater. Chem. A. 2 (2014) 2671–2680. doi:10.1039/c3ta13648e.

[7] P. Barpanda, G. Oyama, C.D. Ling, A. Yamada, Kröhnkite-type $Na_2Fe(SO_4)_2 \cdot 2H_2O$ as a novel 3.25 V insertion compound for Na-ion batteries, Chem. Mater. 26 (2014) 1297–1299. doi:10.1021/cm4033226.

[8] E. Kendrick, J. Kendrick, A. Orera, P. Panchmatia, M.S. Islam, P.R. Slater, Novel aspects of the conduction mechanisms of electrolytes containing tetrahedral moieties, Fuel Cells. 11 (2011) 38–43. doi:10.1002/fuce.201000044.

[9] A. Orera, P.R. Slater, New Chemical Systems for Solid Oxide Fuel Cells †, Chem. Mater. 22 (2010) 675–690. doi:10.1021/cm902687z.

[10] N. Mahato, A. Banerjee, A. Gupta, S. Omar, K. Balani, Progress in material selection for solid oxide fuel cell technology: A review, Prog. Mater. Sci. 72 (2015) 141–337. doi:10.1016/j.pmatsci.2015.01.001.

[11] S.B. Adler, Factors governing oxygen reduction in solid oxide fuel cell cathodes, Chem. Rev. 104 (2004) 4791–4843. doi:Doi 10.1021/Cr020724o.

[12] B.C. Steele, A. Heinzel, Materials for fuel-cell technologies., Nature. 414 (2001) 345–352. doi:10.1038/35104620.

[13] N.Q. Minh, Ceramic Fuel Cells, J. Am. Ceram. Soc. 76 (1993) 563–588. doi:10.1111/j.1151-2916.1993.tb03645.x.

[14] K.J. Lilley, U. Gbureck, A. J. Wright, D.F. Farrar, J.E. Barralet, Cement from nanocrystalline hydroxyapatite: Effect of calcium phosphate ratio, J. Mater. Sci. Mater. Med. 16 (2005) 1185–1190. doi:10.1007/s10856-005-4727-2.

[15] J.E. Barralet, L. Grover, T. Gaunt, A. J. Wright, I.R. Gibson, Preparation of macroporous calcium phosphate cement tissue engineering scaffold, Biomaterials. 23 (2002) 3063–3072. doi:10.1016/S0142-9612(01)00401-X.

[16] G. Buxbaum, G. Pfaff, Industrial Inorganic Pigments, Wiley-VCH, Mörlenbach, 2005.

[17] L.L. Driscoll, E. Kendrick, A.J. Wright, P.R. Slater, Investigation into the effect on structure of oxoanion doping in $Na_2M(SO_4)_2{\cdot}2H_2O$, J. Solid State Chem. 242 (2016) 103–111. doi:10.1016/j.jssc.2016.07.004.

[18] P. Barpanda, G. Oyama, S. Nishimura, S.-C. Chung, A. Yamada, A 3.8-V earth-abundant sodium battery electrode, Nat Commun. 5 (2014). http://dx.doi.org/10.1038/ncomms5358.

[19] G. Oyama, S. Nishimura, Y. Suzuki, M. Okubo, A. Yamada, Off-Stoichiometry in Alluaudite-Type Sodium Iron Sulfate $Na_{2+2x}Fe_{2-x}(SO_4)_3$ as an Advanced Sodium Battery Cathode Material, ChemElectroChem. 2 (2015) 1019–1023. doi:10.1002/celc.201500036.

[20] J. Lu, A. Yamada, Ionic and Electronic Transport in Alluaudite $Na_{2+2x}Fe_{2-x}(SO_4)_3$, CHEMELECTROCHEM. 3 (2016) 902–905. doi:10.1002/celc.201500535.

[21] A.C. Larson, R.B. Von Dreele, General Structure Analysis System (GSAS), Structure.

748 (2004) 86–748. doi:10.1103/PhysRevLett.101.107006.

[22] B.H. Toby, EXPGUI, a graphical user interface for GSAS, J. Appl. Crystallogr. 34 (2001) 210–213. doi:10.1107/S0021889801002242.

[23] D.M. Marinova, E.N. Zhecheva, R.R. Kukeva, P. V. Markov, D.D. Nihtianova, R.K. Stoyanova, Mixed sodium nickel-manganese sulfates: Crystal structure relationships between hydrates and anhydrous salts, J. Solid State Chem. 250 (2017) 49–59. doi:10.1016/j.jssc.2017.03.015.

[24] A.M. Fry, O.T. Sweeney, W. Adam Phelan, N. Drichko, M. a. Siegler, T.M. McQueen, Unique edge-sharing sulfate-transition metal coordination in $Na_2M(SO_4)_2$ (M=Ni and Co), J. Solid State Chem. 222 (2015) 129–135. doi:10.1016/j.jssc.2014.11.010.

[25] F. Cotton, G. Wilkinson, C. Murillo, M. Bochmann, Advanced Inorganic Chemistry, 6th Editio, John Wiley & Sons, 1999.

[26] G. Oyama, H. Kiuchi, S.C. Chung, Y. Harada, A. Yamada, Combined Experimental and Computational Analyses on the Electronic Structure of Alluaudite-Type Sodium Iron Sulfate, J. Phys. Chem. C. 120 (2016) 23323–23328. doi:10.1021/acs.jpcc.6b05569.

[27] S.I. Nishimura, Y. Suzuki, J. Lu, S. Torii, T. Kamiyama, A. Yamada, High-Temperature Neutron and X-ray Diffraction Study of Fast Sodium Transport in Alluaudite-type Sodium Iron Sulfate, Chem. Mater. 28 (2016) 2393–2399. doi:10.1021/acs.chemmater.6b00604.

[28] D. Dwibedi, C.D. Ling, R.B. Araujo, S. Chakraborty, S. Duraisamy, N. Munichandraiah, R. Ahuja, P. Barpanda, Ionothermal Synthesis of High-Voltage Alluaudite $Na_{2+2x}Fe_{2-x}(SO_4)_3$ Sodium Insertion Compound: Structural, Electronic, and

Magnetic Insights, ACS Appl. Mater. Interfaces. 8 (2016) 6982–6991.

doi:10.1021/acsami.5b11302.

Table 1a. Structural parameters for alluaudite-type $Na_3Co_{1.5}(SO_4)_{1.5}(SeO_4)_{1.5}$

Cell parameters: a =11.5822(2) Å, b =12.9486(3) Å, c = 6.6465(1) Å, β = 96.418(2)˚

Cell volume = 990.56(2)Å$^3$

$\chi^2$ = 1.892, wRp = 2.71%, Rp = 3.03%

| Atom type | Site multiplicity | X | y | z | Occupancy | $U_{iso}$*100 (Å$^2$) |
|---|---|---|---|---|---|---|
| Na1 | 4 | 0.245(2) | 0.5178(5) | 0.511(2) | 1.0 | 1.9(2) |
| Na2 | 4 | 0.760(1) | 0.2486(9) | 0.289(2) | 1.0 | 4.2(3) |
| Na3 | 4 | 0.248(4) | 0.265(1) | 0.014(5) | 0.5 | 3.0(5) |
| Co1/Na | 4 | 0.485(1) | 0.091(1) | 0.315(2) | 0.5/0.5 | 2.7(2) |
| Co2 | 4 | 0.0274(1) | 0.410(1) | 0.159(2) | 1.0 | 1.4(2) |
| S1/Se1 | 4 | 0.0106(8) | 0.1425(7) | 0.152(1) | 0.5/0.5 | 1.5(2) |
| O11 | 4 | 0.8816(9) | 0.1658(9) | 0.064(1) | 1.0 | 2.9(3) |
| O12 | 4 | 0.0791(9) | 0.0905(9) | 0.990(1) | 1.0 | 2.6(3) |
| O13 | 4 | 0.0164(9) | 0.0798(9) | 0.342(1) | 1.0 | 1.9(3) |
| O14 | 4 | 0.0690(6) | 0.2505(8) | 0.192(1) | 1.0 | 3.0(3) |
| S2/Se2 | 4 | 0.4879(8) | 0.3532(6) | 0.3634(9) | 0.5/0.5 | 0.3(2) |
| O21 | 4 | 0.4827(9) | 0.4226(9) | 0.164(1) | 1.0 | 2.5(3) |
| O22 | 4 | 0.4169(7) | 0.2559(8) | 0.291(1) | 1.0 | 3.7(3) |
| O23 | 4 | 0.425(1) | 0.4134(9) | 0.517(2) | 1.0 | 3.6(3) |
| O24 | 4 | 0.611(1) | 0.3349(9) | 0.44(1) | 1.0 | 2.5(3) |
| S3/Se3 | 4 | 0.251(1) | 0.5283(3) | 0.991(1) | 0.5/0.5 | 0.52(8) |
| O31 | 4 | 0.1605(8) | 0.6061(7) | 0.894(1) | 1.0 | 3.2(3) |
| O32 | 4 | 0.1981(7) | 0.4521(5) | 0.142(1) | 1.0 | 1.8(2) |
| O33 | 4 | 0.3039(7) | 0.4621(5) | 0.8289(9) | 1.0 | 1.8(2) |
| O34 | 4 | 0.3413(8) | 0.5977(7) | 0.134(1) | 1.0 | 3.0(3) |

Table 1b. Bond lengths for $Na_3Co_{1.5}(SO_4)_{1.5}(SeO_4)_{1.5}$

Na-O bond distances

| Bond | Bond distance (Å) | Bond | Bond distance (Å) | Bond | Bond distance (Å) |
|---|---|---|---|---|---|
| Na1-O11 | 2.431(2) | Na2-O11 | 2.416(2) | Na3-O12 | 2.989(3) |
| Na1-O12 | 2.372(2) | Na2-O11 | 2.447(1) | Na3-O14 | 2.51(4) |
| Na1-O23 | 2.483(2) | Na2-O24 | 2.354(2) | Na3-O14 | 2.82(4) |
| Na1-O24 | 2.529(2) | Na2-O24 | 2.957(1) | Na3-O22 | 2.53(4) |
| Na1-O31 | 3.054(2) | Na2-O31 | 2.875(1) | Na3-O22 | 2.60(4) |
| Na1-O32 | 2.597(1) | Na2-O31 | 2.473(2) | Na3-O23 | 3.091(3) |
| Na1-O33 | 2.266(2) | Na2-O34 | 2.365(2) | Na3-O32 | 2.647(2) |
| Na1-O34 | 3.034(1) | - | - | Na3-O33 | 2.931(2) |
| Average Na1-O | 2.596 | Average Na2-O | 2.555 | Average Na3-O | 2.764 |

S/Se-O bond distances

| Bond | Bond distance (Å) | Bond | Bond distance (Å) | Bond | Bond distance (Å) |
|---|---|---|---|---|---|
| S/Se1 -O11 | 1.570(1) | S/Se2 -O21 | 1.595(1) | S/Se3-O31 | 1.538(1) |
| S/Se1 -O12 | 1.557(1) | S/Se2-O22 | 1.553(1) | S/Se3-O32 | 1.576(1) |
| S/Se1 -O13 | 1.500(1) | S/Se2-O23 | 1.528(1) | S/Se3-O33 | 1.557(1) |
| S/Se1 -O14 | 1.564(1) | S/Se2-O24 | 1.474(1) | S/Se3-O34 | 1.611(1) |
| Average S/Se1 -O | 1.548 | Average S/Se2 -O | 1.538 | Average S/Se3 -O | 1.571 |

Co/Na – O and Co – O bond distances

| Bond | Bond distance (Å) | Bond | Bond distance (Å) |
|---|---|---|---|
| Co1/Na-O21 | 2.220(2) | Co2-O12 | 2.217(2) |
| Co1/Na -O21 | 2.334(2) | Co2-O13 | 2.253(2) |
| Co1/Na -O22 | 2.270(2) | Co2-O13 | 2.099(2) |
| Co1/Na -O23 | 2.025(2) | Co2-O14 | 2.130(2) |
| Co1/Na -O33 | 2.224(2) | Co2-O31 | 2.175(1) |
| Co1/Na -O34 | 2.001(2) | Co2-O32 | 2.067(1) |
| Average Co1/Na-O | 2.179 | Average Co2-O | 2.157 |

Table 2. Cell parameters of phases resulting from the dehydration of

$Na_2Co(SO_4)_{2-x}(SeO_4)_x \cdot 2H_2O$

212 = $Na_2M(SO_4)_2$-type and 223 = alluaudite type phase

| Dopant Level (x) | a (Å) | b (Å) | c (Å) | α (°) | β (°) | γ (°) | Cell vol. ($Å^3$) | Weight % of phase | |
|---|---|---|---|---|---|---|---|---|---|
| | | | | | | | | 212 | 223 |
| 0 | 23.311(2) | 10.3064(8) | 17.406(1) | 90.0 | 98.945(4) | 90.0 | 4131.1(6) | 100 | 0 |
| 0.1 | 23.306(2) | 10.3249(9) | 17.446(2) | 90.0 | 98.880(6) | 90.0 | 4147.9(6) | 78 | 22 |
| | 11.476(2) | 12.705(2) | 6.493(1) | 90.0 | 95.68(3) | 90.0 | 942.2(3) | | |
| 0.25 | 23.28(1) | 10.306(3) | 17.454(9) | 90.0 | 98.81(3) | 90.0 | 4156.0(21) | 15 | 85 |
| | 11.487(1) | 12.751(1) | 6.5227(7) | 90.0 | 95.76(1) | 90.0 | 950.6(3) | | |
| 0.5 | 11.5237(5) | 12.8269(6) | 6.5703(2) | 90.0 | 96.000(4) | 90.0 | 965.9(1) | 0 | 100 |
| 0.75 | 11.5510(5) | 12.8790(5) | 6.6050(2) | 90.0 | 96.197(4) | 90.0 | 976.8(1) | 0 | 100 |
| 1.0 | 11.5822(2) | 12.9487(3) | 6.6466(1) | 90.0 | 96.417(2) | 90.0 | 990.57(2) | 0 | 100 |

Table 3. Cell parameters of phases resulting in the dehydration of $Na_2Ni(SO_4)_{2-x}(SeO_4)_x \cdot 2H_2O$

| Dopant Level (x) | a (Å) | b (Å) | c (Å) | α (°) | β (°) | γ (°) | Cell vol. (Å$^3$) | Weight % of phase 212 | 223 |
|---|---|---|---|---|---|---|---|---|---|
| 0 | 23.196(2) | 10.2577(9) | 17.339(2) | 90.0 | 98.932(6) | 90.0 | 4075.6(7) | 100 | 0 |
| 0.1 | 23.248(1) | 10.2665(6) | 17.374(1) | 90.0 | 98.806(4) | 90.0 | 4098.0(4) | 100 | 0 |
| 0.25 | 23.342(2) | 10.289(1) | 17.420(2) | 90.0 | 98.645(6) | 90.0 | 4136.4(7) | 100 | 0 |
| 0.5 | 23.427(4) | 10.299(2) | 17.468(3) | 90.0 | 98.5(1) | 90.0 | 4168.3(13) | 75 | 25 |
| | 11.556(3) | 12.689(3) | 6.504(2) | 90.0 | 96.27(5) | 90.0 | 947.9(4) | | |
| 0.75 | 23.37(1) | 10.311(5) | 17.441(9) | 90.0 | 98.49(4) | 90.0 | 4158.5(24) | 29 | 71 |
| | 11.5605(1) | 12.760(1) | 6.5490(7) | 90.0 | 96.489(6) | 90.0 | 959.8(3) | | |
| 1.0 | 11.5876(7) | 12.8217(8) | 6.5918(4) | 90.0 | 96.736(5) | 90.0 | 972.6(1) | 0 | 100 |

*The high errors in the cell parameter data, especially for $Na_2M(SO_4)_2$ in bi-phasic samples, reflects the complexity of the resultant structures.

Table 4. Cell parameters of phases resulting from the dehydration of $Na_2Mn(SO_4)_{2-x}(SeO_4)_x \cdot 2H_2O$ (all phases obtained adopted the alluaudite-type structure)

| Dopant Level (x) | a (Å) | b (Å) | c (Å) | α (°) | β (°) | γ (°) | Cell vol. (Å$^3$) |
|---|---|---|---|---|---|---|---|
| 0 | 11.545(2) | 12.935(2) | 6.570(1) | 90.0 | 95.051(5) | 90.0 | 977.4(5) |
| 0.1 | 11.5677(8) | 12.9627(8) | 6.5908(4) | 90.0 | 95.155(4) | 90.0 | 984.3(1) |
| 0.25 | 11.5936(8) | 13.0197(9) | 6.6320(4) | 90.0 | 95.330(5) | 90.0 | 996.7(2) |
| 0.5 | 11.6241(7) | 13.0814(8) | 6.6781(4) | 90.0 | 95.591(4) | 90.0 | 1010.6(2) |
| 0.75 | 11.6498(5) | 13.1337(6) | 6.7132(3) | 90.0 | 95.792(4) | 90.0 | 1021.92(8) |
| 1.0 | 11.6785(7) | 13.1861(7) | 6.7470(3) | 90.0 | 95.981(4) | 90.0 | 1033.3(1) |

Figure 1. Crystal structure of $Na_2Co(SO_4)_2$ (tetrahedra =$SO_4$; Co at the centre of octahedral, spheres = Na)

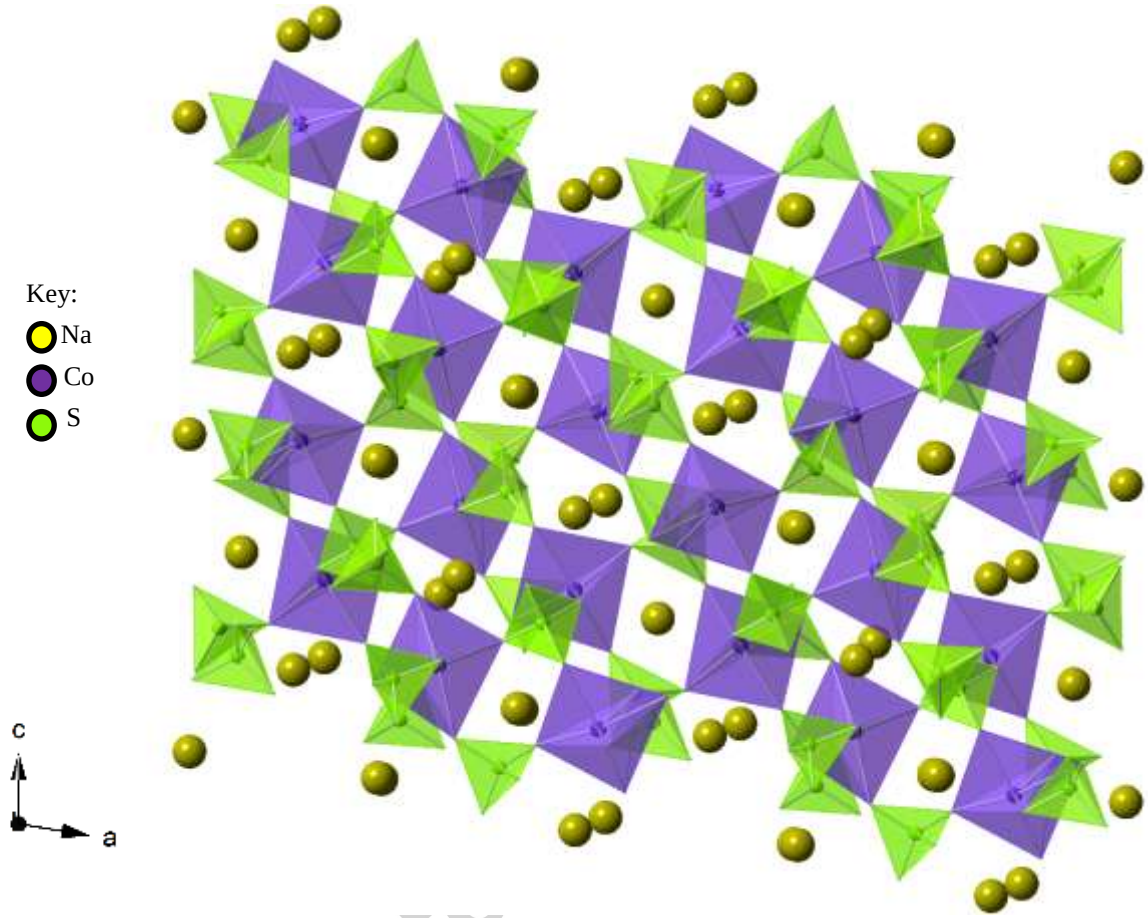

Figure 2. X-ray diffraction patterns obtained after the dehydration of $Na_2Co(SO_4)_{2-x}(SeO_4)_x \cdot 2H_2O$ (Co Kα X-rays) showing the formation of $Na_2Co(SO_4)_2$ (x=0), a mixture of $Na_2Co(SO_4)_2$ and an alluaudite phase for $0.1 \leq x \leq 0.25$, and a single phase alluaudite-type material for $0.5 \leq x \leq 1.0$.

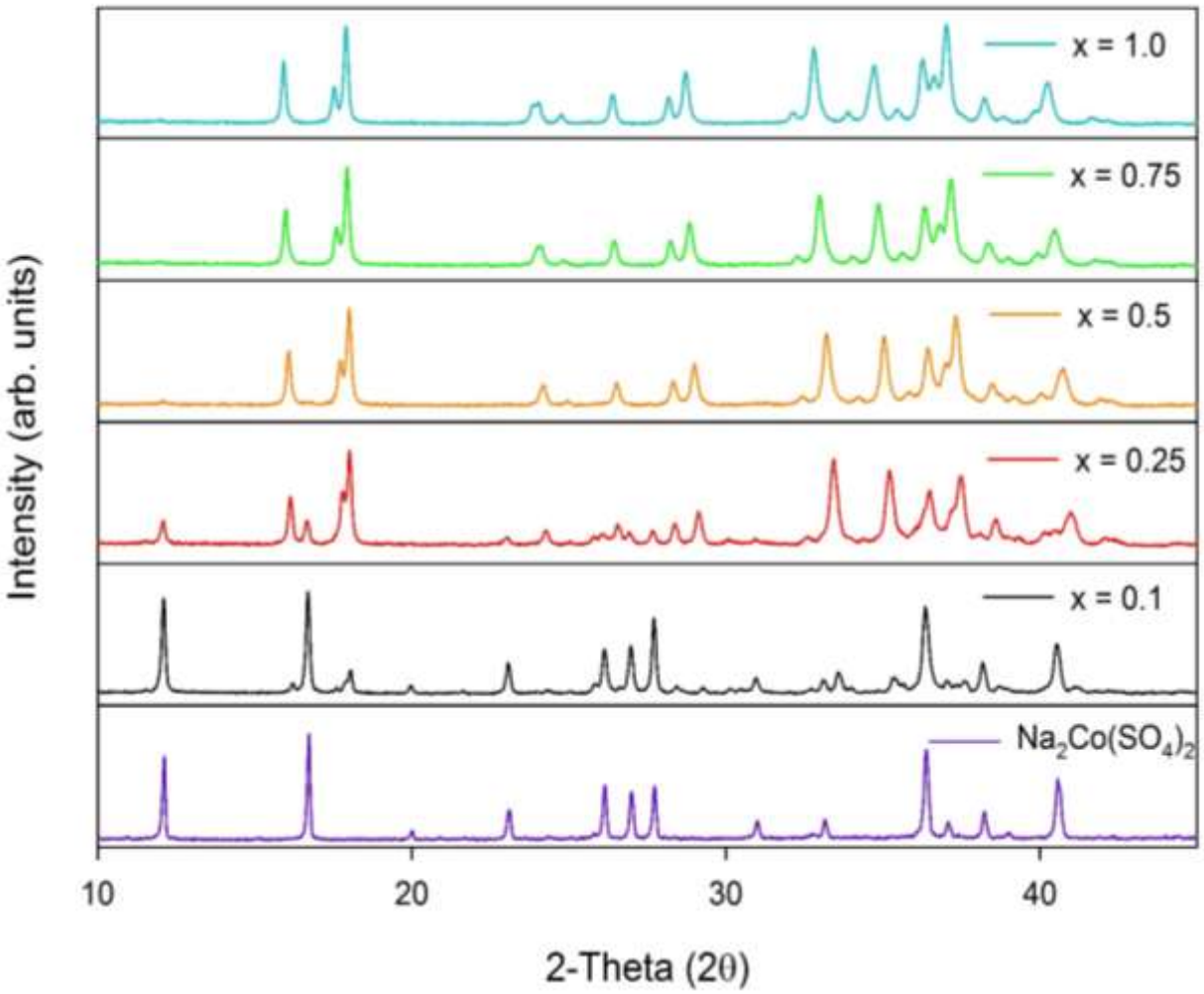

Figure 3. Observed, Calculated and Difference plots for Rietveld analysis of $Na_3Co_{1.5}(SO_4)_{1.5}(SeO_4)_{1.5}$ (Neutron (above), X-ray (Below)/(Co Kα).

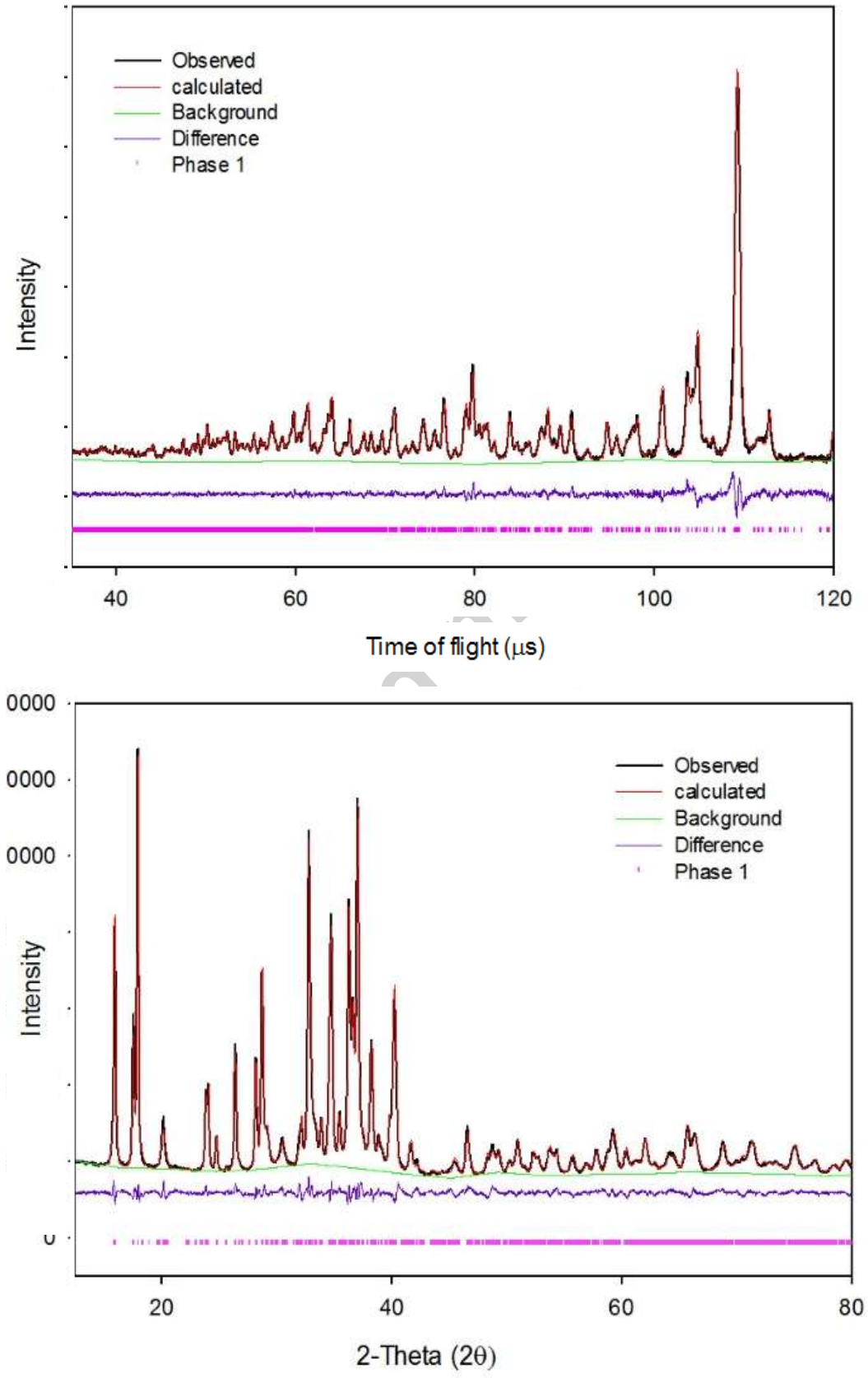

Figure 4. The refined crystal structure of alluaudite-type $Na_3Co_{1.5}(SO_4)_{1.5}(SeO_4)_{1.5}$

(Tetrahedra = $S/SeO_4$; Co (and mixed Co/Na site) at the centre of octahedra, Spheres = Na)

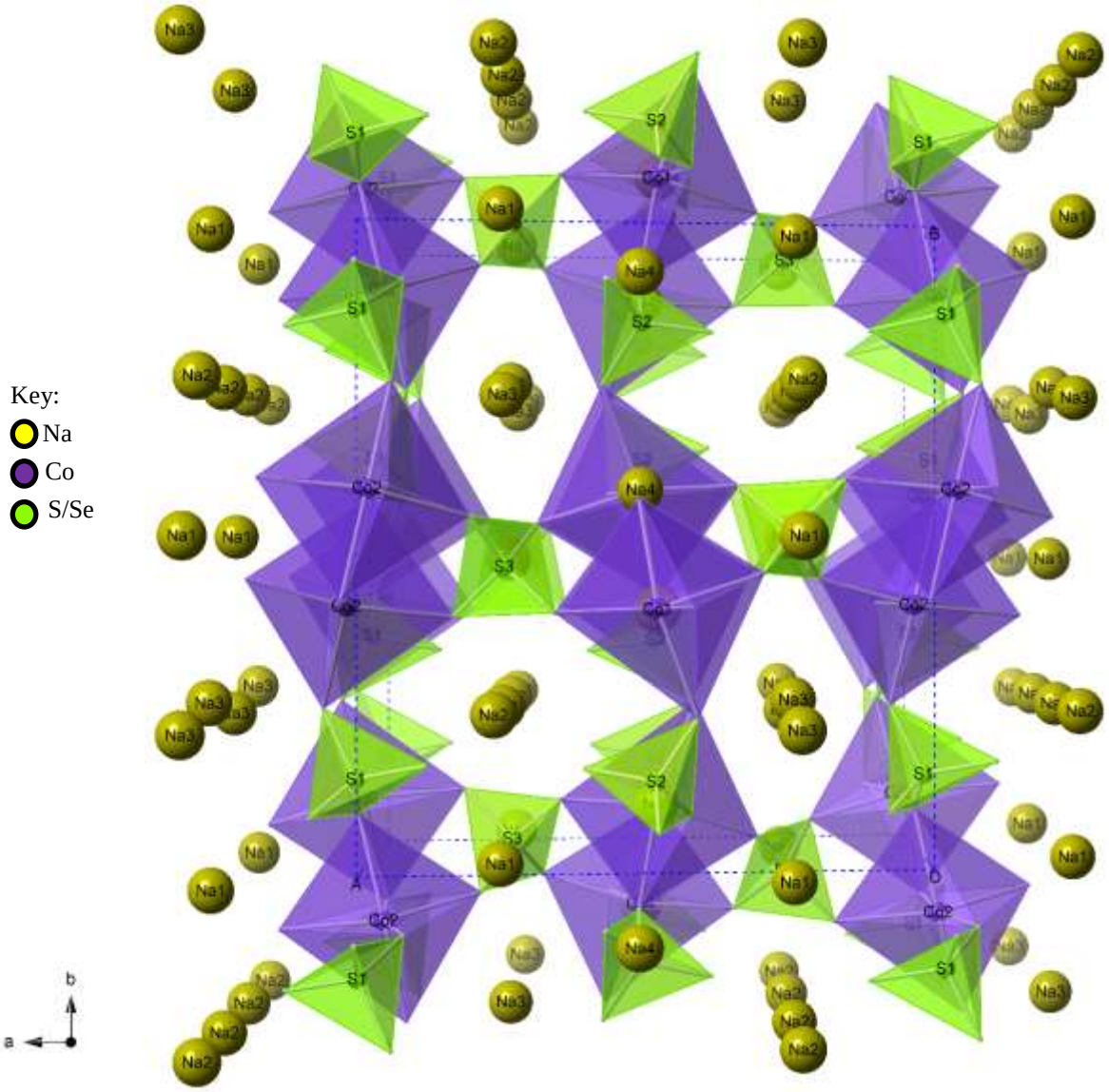

Figure 5. X-ray diffraction patterns obtained from the dehydration of $Na_2Ni(SO_4)_{2-x}(SeO_4)_x \cdot 2H_2O$ (Co Kα1/ Kα2). Additional peaks in the undoped system are attributed to $Na_6Ni(SO_4)_4$ (10wt%), which is not present in any of the selenate doped samples. The X-ray diffraction patterns show the formation of $Na_2Ni(SO_4)_2$ (x=0), a mixture of $Na_2Ni(SO_4)_{2-x}(SeO_4)_x$ and an alluaudite phase for $0.1 \leq x \leq 0.75$, and a single phase

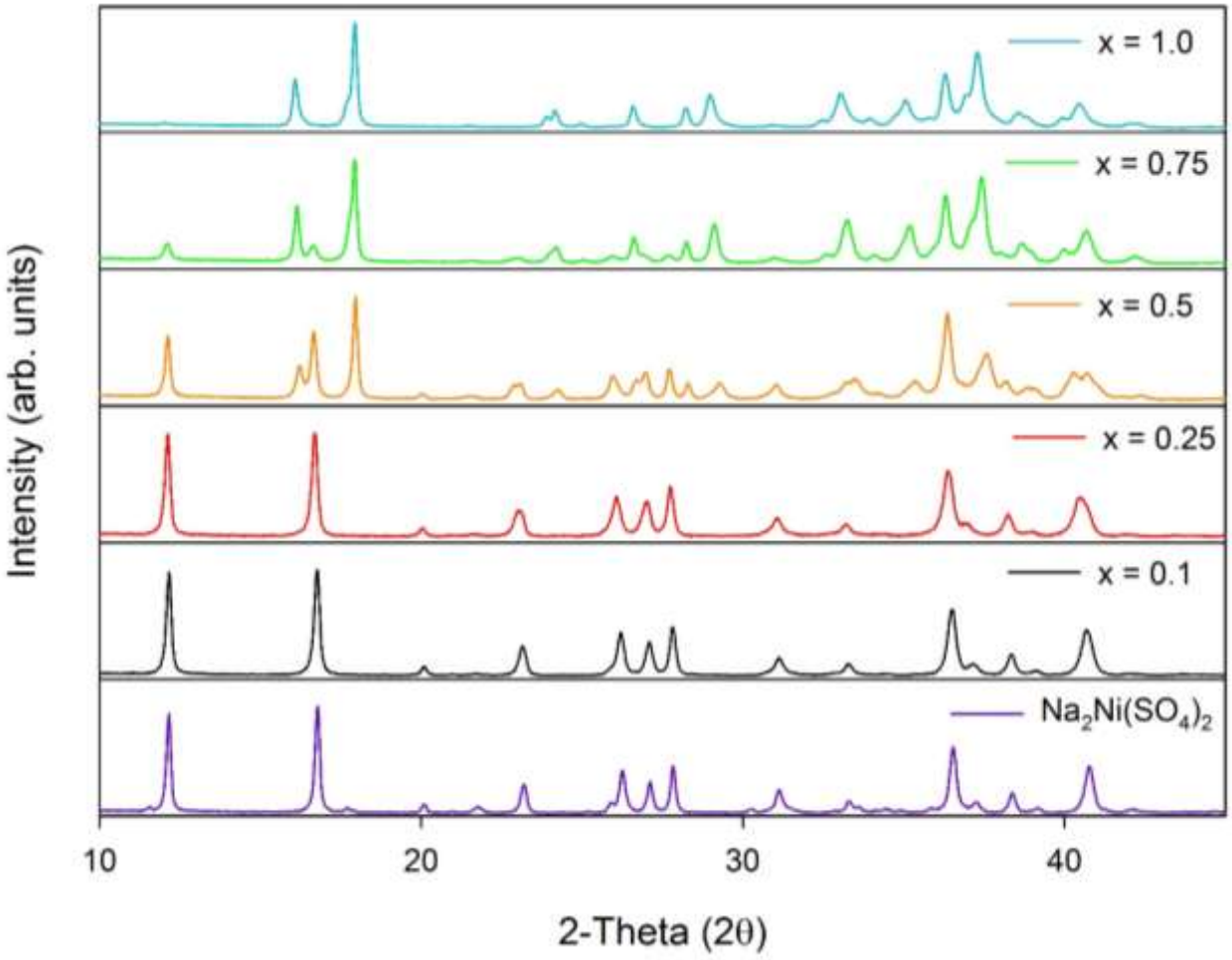


alluaudite-type material for x=1.0.

Figure 6. X-ray diffraction patterns resulting from the dehydration of $Na_2Mn(SO_4)_{2-x}(SeO_4)_x \cdot 2H_2O$ (Cu Kα), showing the formation of an alluaudite phase across the series.

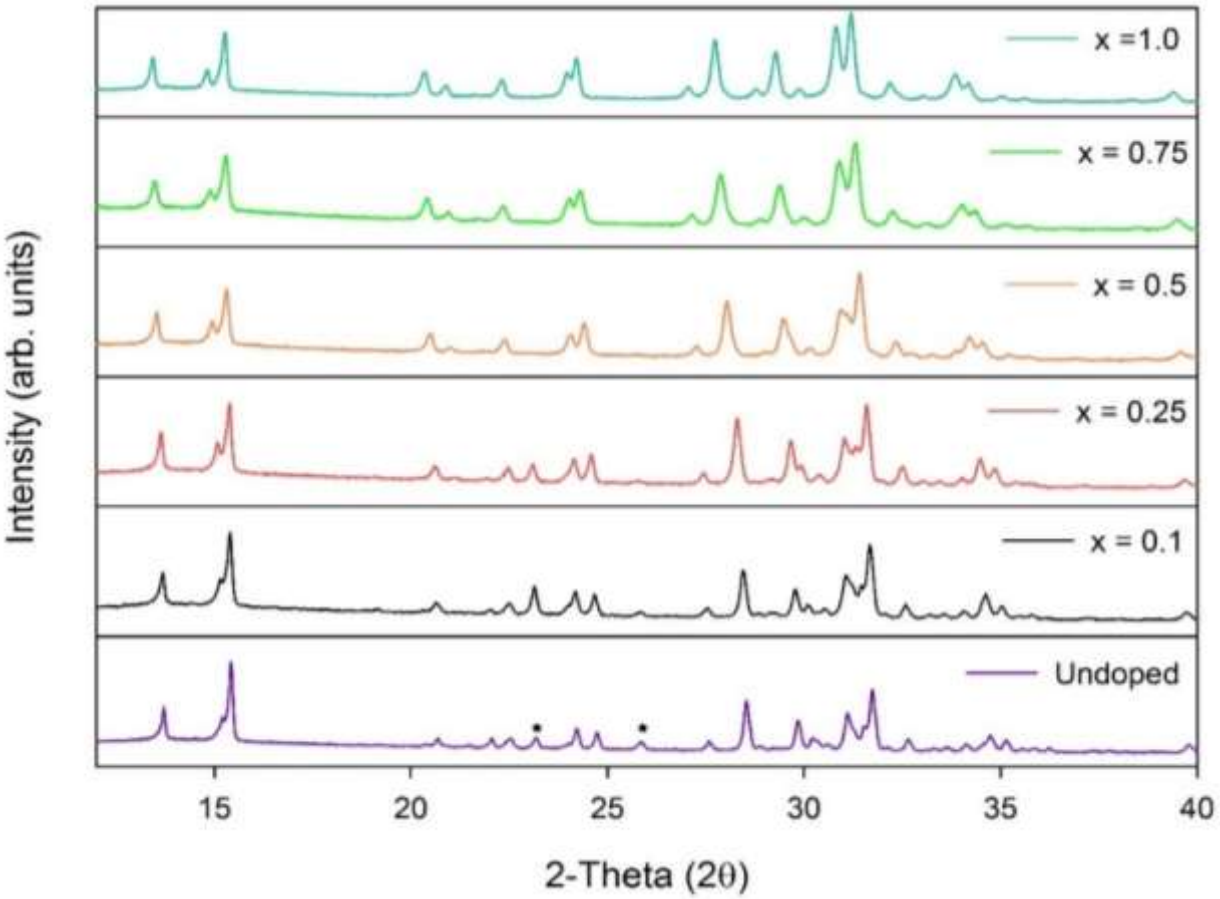

Figure 7. Cell volumes of alluaudite phases plotted against the precursor hydrated material's selenate content ($Na_2M(SO_4)_{2-x}(SeO_4)_x \cdot 2H_2O$).

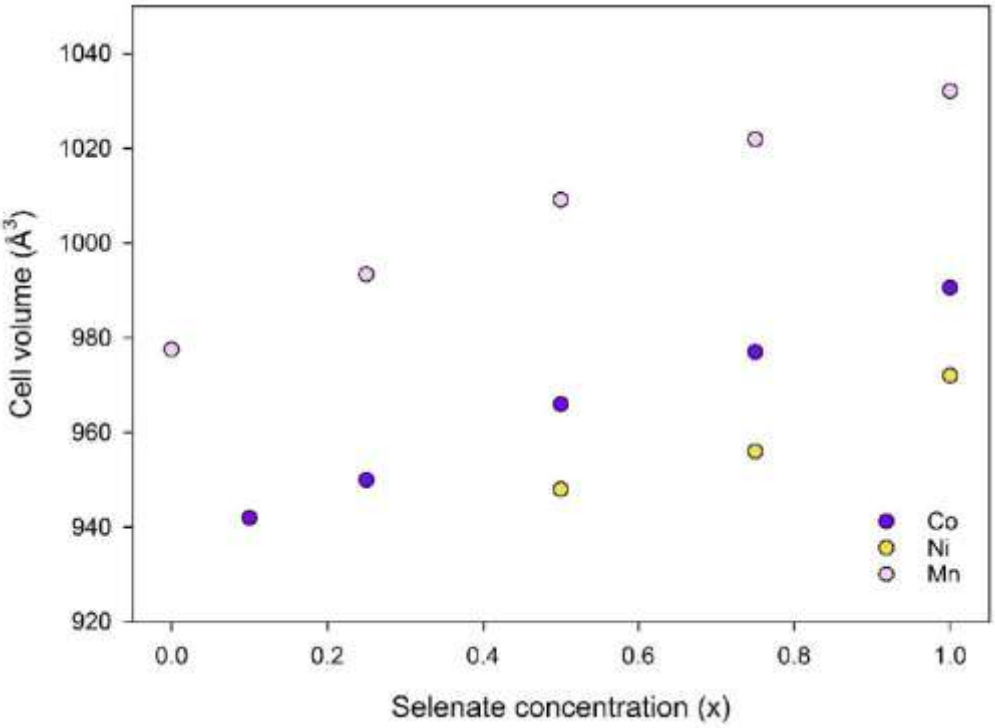

Figure 8. Raman data for phases resulting from the dehydration $Na_2M(SO_4)_{2-x}(SeO_4)_x \cdot 2H_2O$ (Where x = 0-1.0 and M = Mn (Top), Co (Middle) and Ni (Bottom))

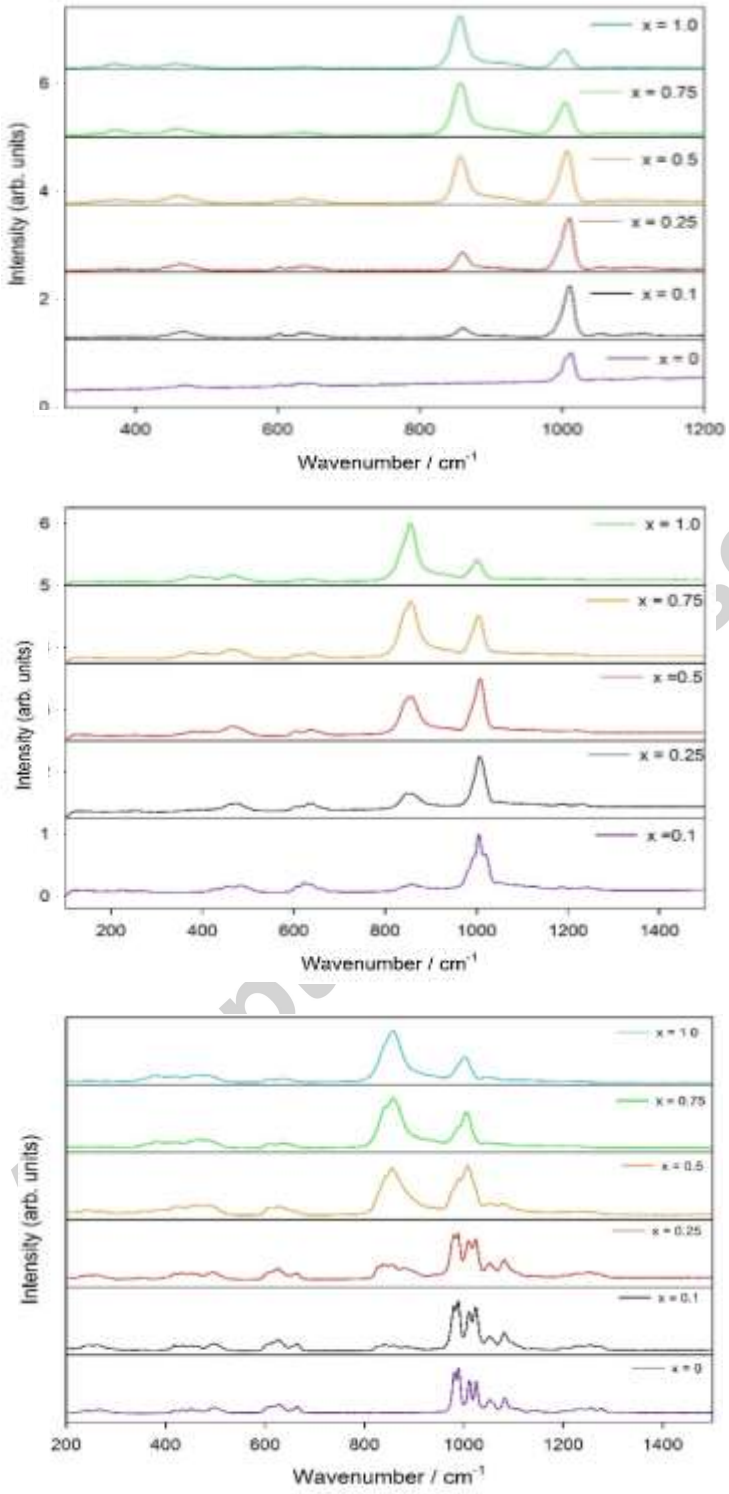

Figure 9. Plot of sum of the ionic radii of M and the weighted average ionic radius of S/Se (where M = Mn, Fe, Co and Ni) vs selenate content in the starting dihydrate. Note only the undoped (no selenate) Fe phase resulted in a crystalline product after dehydration, therefore only one data point is available for this series.

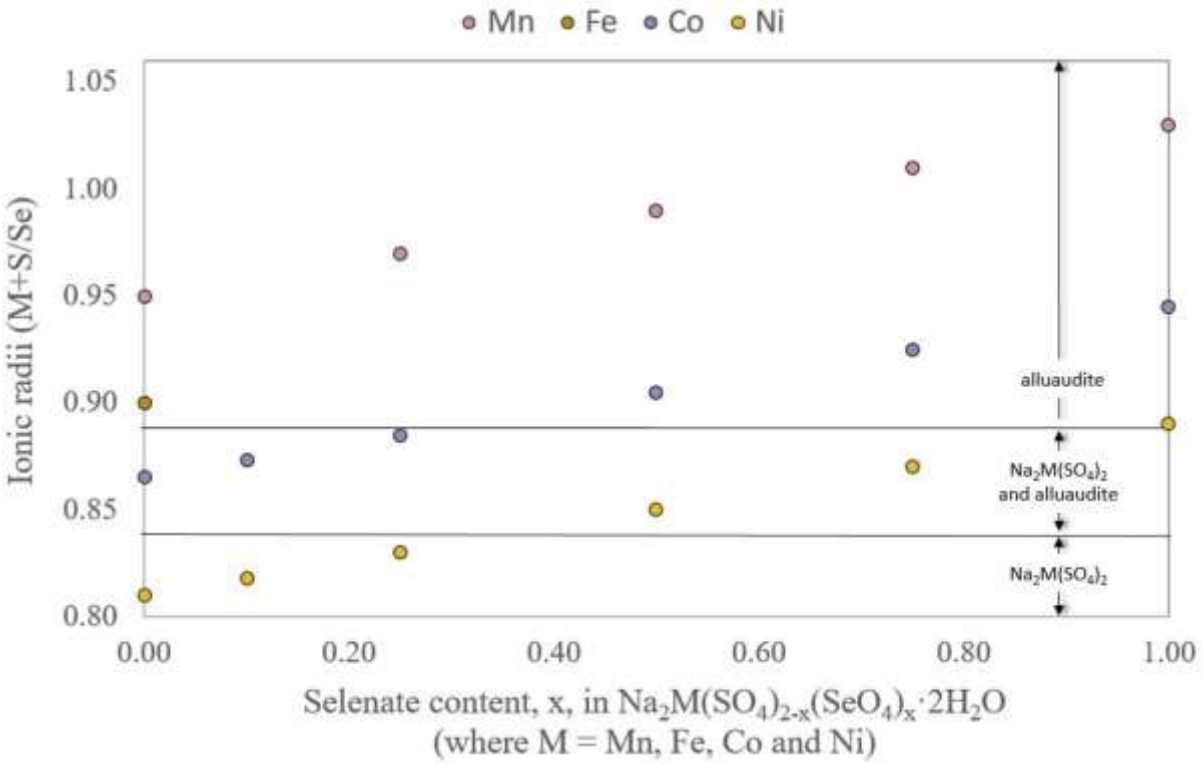

## Graphical abstract

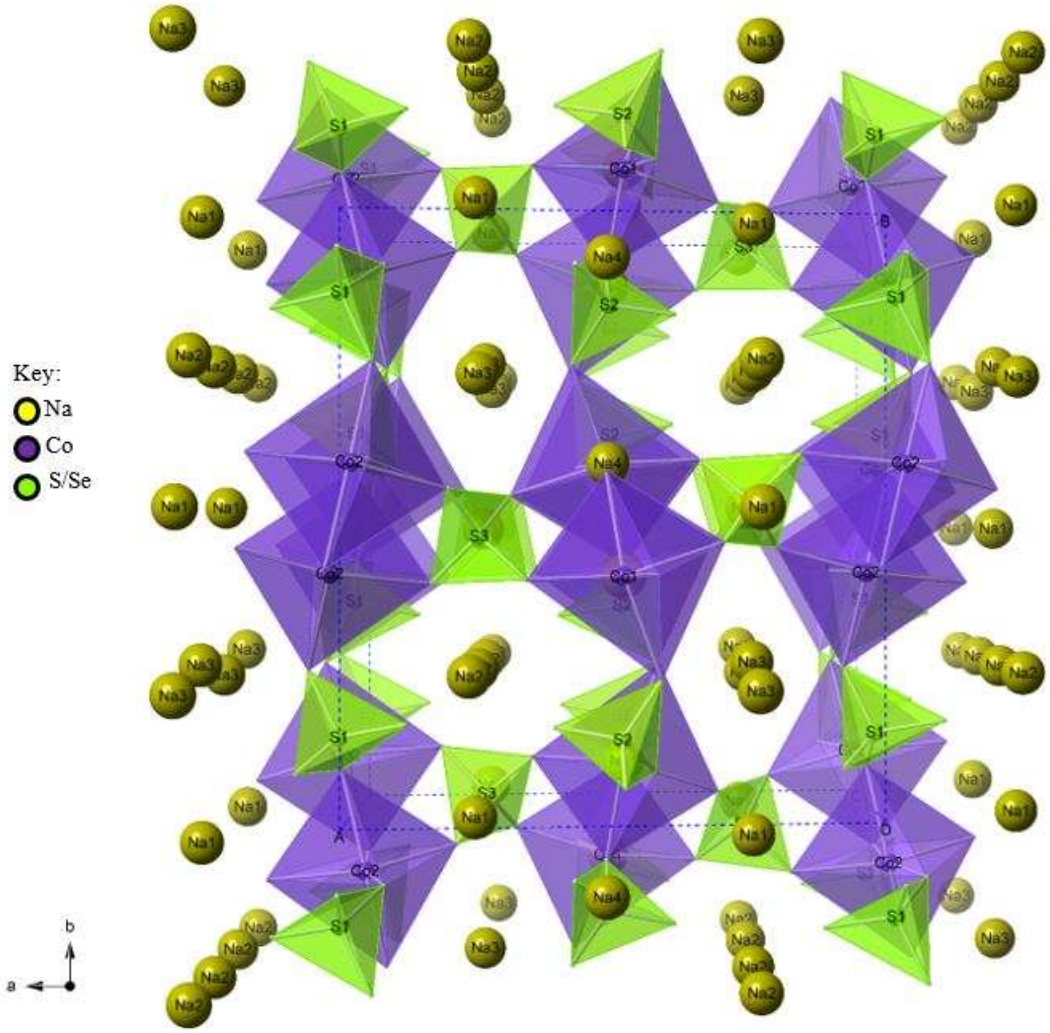


The refined crystal structure of alluaudite-type $Na_3Co_{1.5}(SO_4)_{1.5}(SeO_4)_{1.5}$ (Tetrahedra = $S/SeO_4$; Co (and mixed Co/Na site) at the centre of octahedra, Spheres = Na)

**Highlights:**

- The highest reported sodium content for an alluaudite phase constructed from sulfate/selenate tetrahedra
- The first report of a nickel alluaudite phase